An ultrafast determination of antimicrobial resistant *Staphylococcus aureus* specifically captured by functionalized magnetic nanoclusters

Fei Pan[1, #, *], Stefanie Altenried[1], Subas Scheibler[2, 3], Irene Rodriguez Fernandez[1, †], Giorgia Giovannini[4], Qun Ren[1, *]

[1]Laboratory for Biointerfaces, Empa, Swiss Federal Laboratories for Materials Science and Technology, Lerchenfeldstrasse 5, 9014 St. Gallen, Switzerland

[2]Nanoparticle Systems Engineering Laboratory, Institute of Process Engineering, Department of Mechanical and Process Engineering, ETH Zürich, Sonneggstrasse 3, 8092 Zürich, Switzerland

[3]Laboratory for Particles Biology Interactions, Empa, Swiss Federal Laboratories for Materials Science and Technology, Lerchenfeldstrasse 5, 9014 St. Gallen, Switzerland

[4]Laboratory for Biomimetic Membranes and Textiles, Empa Swiss Federal Laboratories for Materials Science and Technology, Lerchenfeldstrasse 5, 9014 St. Gallen, Switzerland

*Correspondence: fei.pan@empa.ch (F.P.); qun.ren@empa.ch (Q.R.)

[#]Present address: Department of Chemistry, University of Basel, Mattenstrasse 24a, BPR 1096, 4058 Basel, Switzerland. (fei.pan@unibas.ch)

[†]Present address: Photon Science Division, Paul Scherrer Institut (PSI), Forschungsstrasse 111, 5232 Villigen, Switzerland

ABSTRACT

Sepsis, the systemic response to infection, is a life-threatening situation for a patient and leads to high mortality, especially when caused by antimicrobial resistant pathogens. Prompt diagnosis and identification of the pathogenic bacteria, including their antibiotic resistance, are highly desired to yield a timely decision for treatment. Here, we aim to develop a platform for rapid isolation and efficient identification of *Staphylococcus aureus*, the most frequently occurring pathogen in sepsis. A peptide (VPHNPGLISLQG, SA5-1), specifically binding to *S. aureus,* was conjugated to the PEGylated magnetic nanoclusters, successfully enabling specific capture and enrichment of *S. aureus* from blood serum. Consequently, fast detection of the antimicrobial resistance of the collected *S. aureus* was achieved within 30 min by a novel luminescent probe. These magnetic nanoclusters manifest a promising diagnostic prospect to combat sepsis.

Keywords: Sepsis, *Staphylococcus aureus*, Antimicrobial resistance, Specific capture, Rapid detection

Introduction

Given the clinical symptoms of sepsis, indistinguishable from those of the non-infectious systemic inflammatory response syndrome[1], an accurate and rapid diagnosis of sepsis becomes extremely challenging. The very low bacterial concentration in the infected bloodstream of a patient (often <10 colony forming units (CFU) $\cdot mL^{-1}$) requires a long culture time and yields a notoriously high chance of false negatives[2]. The diagnostic ambiguity, combined with the emergence of pathogens with antimicrobial resistance (AMR), leads to the abuse of antibiotics and failure of antibiotic treatment. *Staphylococcus aureus* infections are one leading cause of sepsis amongst *Escherichia coli*, *Pseudomonas aeruginosa*, and other bacterial pathogens[3], which is even more critical to handle clinically once antimicrobial resistance evolves [4, 5].

Many efforts have been dedicated to achieving a fast diagnosis of antimicrobial resistance and its effective treatments, such as using single-cell morphological analysis[6] and localized surface plasmon resonance[7]. Despite the substantial advances made, antimicrobial resistance diagnostics still face huge challenges. One of the challenges is the long turnaround time, particularly for blood samples. Currently, the gold standard for the antimicrobial susceptibility test (AST) of blood sepsis relies on blood culture, which requires three overnight culture steps: blood culture to enrich bacterial cells, subculture on an agar plate to obtain pure bacterial colonies, and AST culture using pure bacterial stock, and takes 48 - 72 h (or longer for fastidious organisms). Almost all novel technologies reported still require cultivation steps to enrich the microbes present and purify them. To be truly rapid, workflows should test non-cultured clinical samples directly. To do this, methods must be developed to eliminate the majority of blood cell components while maintaining the integrity of the infective microbes. Different approaches have been reported, such as using selective lysis followed by centrifugation [8] or spin column purification[9], centrifugal gradients followed by filtration[10-12], or microfluidic devices to separate bacteria from the majority of blood components[13, 14]. However, these techniques are limited by poor bacterial recovery, damaged bacterial cells due to usage of toxic reagents, or additional time for further growth[9, 15-17]. Antibodies have also been used to recover bacteria due to their high specificity toward target antigens on the surfaces of pathogens[18]. However, the antibody preparation is complex and costly, and very few antibodies for specific targets are available[19]. Furthermore, antibodies are usually very large and difficult to immobilize on a given surface, especially a sphere surface, limiting their widespread applications in particle-based pathogenic bacteria detection[19]. Apart from antibodies, some antibiotics, proteins (such as avidin, biotin, lectin, *et al*.), DNA/RNA aptamers, and carbohydrates (such as glycan) have also been used as targeting ligands to probe target bacteria[20]. However, poor specificity is one of the general problems.

Magnetic particles have also been used for blood purification due to their controllable collection of bacterial pathogens[21, 22], which is difficult to achieve by the current blood purification systems, such as hemofiltration and hemosorption. However, the low specificity of the capturing function restrains the clinical translation of such magnetic separation[21]. Hence, it is urgently needed to develop a capturing platform that can specifically select the desired pathogen of extremely low concentration to allow rapid pathogen identification and AMR determination. Various biomolecules have been exploited to bestow a material affinity towards bacteria, *e.g.*, carbohydrates, lectins, or adhesins[23], but such molecules cannot recognize a certain species of bacteria for a specific bacterial capture. To this end, phage display of random peptide libraries and phage-display panning method have been used to identify a peptide that can specifically bind to a target of interest[24, 25]. Since the bacterial surface displays unique molecular compositions, a well-selected peptide can interact with an epitope or receptor, yielding a highly specific binding[26, 27]. The extraordinary specificity nature of the binding peptides toward its

host, combined with magnetic particles, will allow direct capture of the targeted pathogens and the subsequent purification and enrichment *via* a magnetic field in a single step. The VPHNPGLISLQG (SA5-1) peptide was thereby identified to bind specifically to the cell surface of *S. aureus*[27]. Herein, we further utilized the SA5-1 peptide to functionalize magnetic particles for specific capture and enrichment of *S. aureus*, followed by fast detection of pathogens and AMR using a colorimetric method.

Results and Discussion

The SA5-1 peptide was first conjugated to the commercially purchased PEGylated magnetic nanoclusters (PEG@MNCs) *via* the covalent bonding between -COOH of the peptide and -NH_2 of the nanoclusters. Different concentrations of SA5-1 peptides were applied for the conjugation. Based on the X-ray photoelectron spectroscopy analysis, the [C]/[O] elemental ratio of 75.0 ± 0.5 %, 264.0 ± 1.6 %, 296.8 ± 6.4 %, 309.5 ± 4.4 % and 314.4 ± 9.0 % was obtained for the SA5-1 initial concentration of 0.02, 0.2, 1, 2 and 20 mM, respectively (Figure 1a). Considering the similarly high [C]/[O] ratio for 2 and 20 mM SA5-1 and the cost of the peptide, PEG@MNCs modified with 2 mM SA5-1 (peptide@PEG@MNCs) were used in the subsequent studies (Figure 1b&S1a).

According to the dynamic light scattering measurement, the obtained peptide@PEG@MNCs exhibited a size (in diameter) of 150.8 ± 1.8 nm (Figure S1b), slightly larger than the naked PEG@MNCs of 142.3 ± 0.9 nm (Figure S1 a&b). The transmission electron microscopy (TEM) images showed the nanoparticles formed clustered (Figure 1b &S1a); therefore, they are named nanoclusters in this work. Moreover, the peptide@PEG@MNCs and PEG@MNCs both displayed magnetic properties and no cytotoxicity at the concentrations studied (Figure S1c&d). To investigate the detection limit of peptide@PEG@MNCs, different concentrations of bacterial solutions were applied, using susceptible *S. aureus* as a model. The peptide@PEG@MNCs successfully captured the *S. aureus* cells even in an extremely low concentration range of 10^0 CFU·mL^{-1}. The capture efficiency was reduced when bacterial concentration rose above 10^6 CFU·mL^{-1} (Figure 1c). Thus, bacterial concentrations below 10^6 CFU·mL^{-1} were applied in the following study. To demonstrate the specificity of the peptide@PEG@MNCs, different bacterial strains with a concentration of about 10^5 CFU·mL^{-1} were assessed, including *E. coli*, *P. aeruginosa*, susceptible and resistant *S. aureus*, and *S. epidermidis* (Figure 1d). More than 70 % of the capture efficiency was obtained for all the tested bacteria within 10 minutes, suggesting that peptide@PEG@MNCs can efficiently remove bacteria from the contaminated system (Figure 1d). To avoid the non-specific binding of bacteria, the rinsing process was introduced to reduce and prevent the interference of non-specific interaction. Using *E. coli* and susceptible *S. aureus* as examples, a five-time rinsing process led to the disappearance of *E. coli* from the collected peptide@PEG@MNCs, but still about 40 % of capture efficiency for *S. aureus* (Figure 2a). The attachment of the susceptible *S. aureus* to the peptide@PEG@MNCs after five-time rinsing can also be clearly seen by TEM analysis (Figure S1e&f). Therefore, the fabricated peptide@PEG@MNCs, on the one side, can specifically capture *S. aureus* after applying the rinsing process. On the other side, it enables the isolation of various bacterial pathogens without rinsing steps (Figure 1d&2a).

The specificity of peptide@PEG@MNCs capture with a rinsing process was further evaluated for *S. aureus* (both susceptible and resistant), *S. epidermidis*, *P. aeruginosa,* and *E. coli* using MNCs, PEG@MNCs, and peptide@MNCs as controls (Figure 2). Capture was only found for susceptible and resistant *S. aureus* incubated with the peptide@PEG@MNCs, whereas applying other strains and nanoclusters did not result in detectable capture (Figure 2b). In order to gain a better understanding of the interaction between the various bacterial pathogens and

the nanoclusters, single-bacteria force spectroscopy was exploited to quantify the affinity between individual bacteria and the nanoclusters (Figure 2c and Table 1). In the measurement, the nanoclusters were immobilized through polydopamine on the petri dish, as reported previously[28]. The average adhesion force of all the tested bacteria strains towards the MNCs and peptide@MNCs was very similar and in the range of 0.50 - 2.30 nN. The affinity of the tested strains towards the PEG@MNCs was measured to be even lower, in a range of 0.40 - 0.55 nN average adhesion force, which was probably caused by the antifouling property of PEG, a well-known feature of PEG[29]. Interestingly, the tested strains manifested different affinity towards the peptide@PEG@MNCs with the average single bacterial adhesion forces for *E. coli*, *S. epidermidis,* and *P. aeruginosa* in a range of 1.04 - 2.69 nN, and for *S. aureus* (both susceptible and resistant) at 24.46 and 15.50 nN, respectively. These results clearly demonstrated a comparatively strong binding of the functionalized PEG@MNCs to *S. aureus*, explaining why only *S. aureus* was captured by the peptide@PEG@MNCs (Figure 2b). The specific capture efficacies towards susceptible and resistant *S. aureus* were lost after rinsing, namely, from over 80 % (Figure 1d) to 37.6 ± 0.6 % and 17.2 ± 1.0 %, respectively (Figure 2d). Thereby, the designed peptide@PEG@MNCs can yield a specific capture towards *S. aureus* through strong attachment to the bacterial surface.

To discover the optimal interaction time, the interaction between the peptide@PEG@MNCs and *S. aureus* was conducted for 5, 10, 30, 60, 90, and 120 min in phosphate buffer saline (PBS) (Figure 2d). It was observed that 10 min incubation was sufficient to reach the optimized interaction time between the peptide@PEG@MNCs and *S. aureus*, and further incubation up to 120 min had almost no impact on the capture efficiency.

To further analyze the sensitivity of the peptide@PEG@MNCs with rinsing steps towards *S. aureus,* different concentrations (10^0-10^5 CFU·mL^{-1}) of *S. aureus* were assessed (Figure 2e). Both susceptible and resistant *S. aureus* could be recovered by the peptide@PEG@MNCs, even at an extremely low concentration of bacteria (10^0 CFU·mL^{-1}, Figure 2e), indicating that the designed peptide@PEG@MNCs can yield a specific capture of *S. aureus* with high sensitivity. We also noticed that the specific capture towards resistant *S. aureus* was comparatively lower than the susceptible one, probably due to the relatively lower affinity between the peptide@PEG@MNCs and resistant *S. aureus* (Figure 2c&e and table 1).

To demonstrate the efficacy of the fabricated peptide@PEG@MNCs under conditions simulating a sepsis situation, human serum spiked with *S. aureus* was utilized. The capture efficiency without a rinsing process reached as high as 82.7 % and 75.0 % for susceptible and resistant *S. aureus*, respectively (Figure 3a). The captured *S. aureus* was subsequently analyzed for antimicrobial resistance by employing the AquaSpark luminescent dye (Figure 3b) and optical density measurement (Figure S2a&b): the former allowed an observation of clearly different growth behavior of susceptible and resistant *S. aureus* after incubation for 30 min in the presence of antibiotic vancomycin, which the conventional OD measurement cannot notice. The fabricated peptide@PEG@MNCs thus enabled a rapid determination of antimicrobial resistance within 30 min through the luminescent analysis. To further demonstrate the specificity of the peptide@PEG@MNCs towards *S. aureus* with a rinsing process, the human serum spiked with *S. aureus,* and one of *S. epidermidis*, *P. aeruginosa,* and *E. coli* was analyzed. Bacterial recovery was only found for *S. aureus* (Figure 3c&d). The capture efficiency of about 15.0 % and 10.8 % was obtained for the samples containing susceptible and resistant *S. aureus*, respectively, regardless of the presence or absence of other bacterial strains. To confirm whether the captured bacteria from a suspension of *S. aureus* mixed with *E. coli* or *P. aeruginosa* are *S. aureus*, the polymerase chain reaction (PCR) analysis was performed, and the results demonstrated that only *S. aureus* was isolated from the human serum spiked with

various bacterial pathogens (Figure S3). Therefore, the fabricated peptide@PEG@MNCs are able to specifically capture *S. aureus* from an infected media containing single or mixed bacterial pathogens.

The captured *S. aureus* was next analyzed for their antimicrobial resistance in the presence of antibiotics, *e.g.*, vancomycin, using a luminescence-based assay (Figure 3e) and optical density measurement (Figure S2c-f). After incubation for 180 minutes, the luminescent intensity displayed a discrepancy for nanoclusters containing resistant and susceptible *S. aureus* (Figure 3e). However, the conventional analysis by optical density did not lead to a measurable discrepancy for those samples (Figure S2c-f). Therefore, susceptible *S. aureus* could be differentiated from the resistant ones within 180 min by utilizing the luminescence-based assay, overcoming the bottleneck arising from the conventional optical density measurement.

CONCLUSIONS

Herein, we demonstrated that the PEGylated MNCs functionalized with SA-5 peptide (peptide@PEG@MNCs) could be applied to isolate various bacterial pathogens, particularly for specific capture of *S. aureus* in an extremely low concentration. The specific capture of *S. aureus* is expected to originate from the comparatively strong affinity between the peptide@PEG@MNCs and the assessed *S. aureus* pathogens. The capture of *S. aureus* in the spiked human serum without a rinsing processing can be as high as 82.7 % and with a rinsing process 15.0 %. The captured *S. aureus* can further be rapidly analyzed (within 180 min) for their antimicrobial resistance through a luminescence method. These results suggest a promising theranostic application of the peptide@PEG@MNCs to remove bacterial pathogens from the blood of sepsis patients, identify the existence of *S. aureus,* and lead to a fast determination of antimicrobial resistance towards *S. aureus*. This work demonstrated theranostic potential to treat sepsis and a concept that can solve other challenges, *e.g.*, urinary infections and water contaminations.

MATERIALS AND METHODS

Materials. Chemicals and reagents were provided with analytical purity from Sigma-Aldrich (Buchs, Switzerland) and utilized as received unless otherwise specified. Dextran iron oxide composite clusters (MNCs, Product code: 09-00-132, 25 $g \cdot L^{-1}$, 130 nm) and PEG-NH_2 functionalized dextran iron oxide composite nanoclusters (PEGylated MNCs, Product code: 09-55-132, 10 $g \cdot L^{-1}$, 130 nm) were purchased in aqueous suspension from micromod Partikeltechnologie GmbH (Rostock, Germany). Phosphate-buffered saline (PBS) at pH 7.4 was prepared as follows: 8 $g \cdot L^{-1}$ NaCl, 0.2 $g \cdot L^{-1}$ KH_2PO_4, and 1.44 $g \cdot L^{-1}$ Na_2PO_4 in distilled water. Bacterial growth medium (LB broth) was prepared: 10 $g \cdot L^{-1}$ tryptone, 5 $g \cdot L^{-1}$ yeast extract, and 5 $g \cdot L^{-1}$ NaCl in distilled water. Broth media adjusted to pH 7.4 was prepared: 5 $g \cdot L^{-1}$ peptone, 5 $g \cdot L^{-1}$ NaCl, 2 $g \cdot L^{-1}$ yeast extract, 1 $g \cdot L^{-1}$ beef extract. Sterile-filtered human serum (Product Number: H4522, from human male AB plasma, USA origin, sterile-filtered) was purchased from Sigma-Aldrich (Buchs, Switzerland). PC-agar plates were prepared: 12.0 $g \cdot L^{-1}$ agar, 1.0 $g \cdot L^{-1}$ dextrose, 5.0 $g \cdot L^{-1}$ tryptone, and 2.5 $g \cdot L^{-1}$ yeast extract. Trizma Buffer (pH 7.0) was prepared: 1.011 $g \cdot L^{-1}$ Trizma Hydrochloride and 11.337 $g \cdot L^{-1}$ Trizma Base.

Functionalization kinetics of magnetic nanoclusters. A peptide (VPHNPGLISLISLQG, final concentrations of 0.02 mM, 0.2 mM, 1 mM, 2mM, and 20 mM, respectively) specific to *S.aureus*, selected from a bacteriophage display library[27, 30], was added to the MNCs and PEGylated MNCs at a final concentration of 9 $g \cdot L^{-1}$ for both cluster types. Suspensions were shaken at 100 rpm and 25 °C for 2 hours. The clusters in each suspension were subsequently

harvested through three centrifugation repeats at 14000 rpm (20800 rcf) and 25 °C. After each centrifugation step, the supernatant was replaced by the same amount of fresh PBS, and functionalized MNCs were resuspended.

XPS analysis. An X-ray photoelectron spectroscopy (XPS, PHI 5000 VersaProbe II instrument with a monochromatic AlKα X-ray source, USA)[31, 32] was employed to evaluate the surface chemical properties of the samples[33].

Vibrating Sample Magnetometry. Vacuum-dried (0.01 mbar) samples were added into polymer-sample holders and analyzed by vibrating sample magnetometry (VSM) at 300 K by using the physical properties measurement system (PPMS, Version P525, Quantum Design GmbH, Germany) of Quantum Design up to a magnetic field of 3T.

Dynamic light scattering (DLS). Hydrodynamic size and zeta potential of different MNC samples were analyzed by employing a DLS instrument (ZetaSizer90, Malvern) at the refractive index of iron oxide particles (n = 2.918)[34]. Particle suspensions were diluted to a final concentration of 0.1 $g \cdot L^{-1}$ and were briefly sonicated for 30 s before analysis. Each sample was measured in PBS with an established stabilization time of 30 seconds.

TEM analysis. TEM analysis was carried out using a JEOL TEM equipped with an in-column Omega-type energy filter (JEM-2200FS, Joel, Japan)[35-38]. MNCs at 9 $g \cdot L^{-1}$ were diluted 10 times, and 5 µL[39] were added onto a TEM grid (Carbon Film Supported Copper Grid, 200 Meshes, Electron Microscopy Sciences, USA) till the solvent had completely evaporated[39-43].

Cytotoxicity analysis. The cytotoxic analysis of the PEG@MNCs and peptide@ PEG@MNCs was exerted towards normal human dermal fibroblasts (nHDFs, female, caucasian, skin/temple, PromoCell, C-12352). Each sample was centrifugated, and the supernatant was replaced with DMEM (Dulbecco's Modified Eagle Medium) containing 1 % penicillin/streptomycin/neomycin (PSN) to reach a final concentration of 9 $g \cdot L^{-1}$ regarded as no dilution for later analysis meanwhile, in addition to the empty wells (negative control), each sample and its further dilutions (2X, 4X, 8X, 16X, 32X, 64X, and 128X) were tested. Every well (TPP, Trasadingen, Switzerland) was seeded with 10 000 nHDFs in 100 µL DMEM containing 10 % foetal calf serum (FCS) for 24 hours before incubating with the sample solutions. The nHDFs subsequently interacted for 24 hours with 100 µL sample solution (final concentration: 95 %) added with FCS. The nHDFs viability from the negative control was set as 100 %, and cells treated with 1 % Triton X-100 in DMEM containing 5 % FCS were defined as the positive control. The nHDFs viability was determined by employing the MTS [(3-(4,5-Dimethylthiazol-2-yl)-5-(3-carboxymethoxyphenyl)-2-(4-sulfophenyl)-2H-tetrazolium)] assay through the absorbance at 490 nm to assess the metabolic activity of the nHDFs[44-46].

Preparation of bacteria. *Escherichia coli* DSMZ 30083, *Pseudomonas aeruginosa* DSMZ 1117, *Staphylococcus aureus* ATCC 6538, *Staphylococcus aureus* VISA PC3, *Staphylococcus epidermidis* ATCC 49461 were utilized in the bacterial capture assays. A bacteria colony of each bacterial strain from an agar plate was incubated in 10 mL LB in a 50 mL Falcon tube at 160 rpm and 37 °C overnight. 100 µL overnight culture was added into 10 mL fresh LB and subsequently cultivated for approximately 2 h to reach exponential growth as established by empirical analysis through OD measurements.

Antimicrobial resistance (AMR) detection. *S. aureus* ATCC 6538 and *S. aureus* VISA PC3 were incubated in 10 mL LB containing 5 $\mu g \cdot mL^{-1}$ vancomycin in a 50 mL Falcon tube at 160 rpm and 37 °C overnight to determine bacterial sensitivity and resistance to vancomycin. The

overnight bacterial culture of *S. aureus* ATCC 6538 and *S. aureus* VISA PC3 in LB containing 5 $\mu g \cdot mL^{-1}$ vancomycin displayed a clear and turbid bacterial suspension, respectively. Hence, *S. aureus ATCC 6538* and *S. aureus* VISA PC3 have been confirmed susceptible and resistant to vancomycin, respectively. Therefore, in the following, *S. aureus* ATCC 6538 is termed susceptible *S. aureus*, and *S. aureus* VISA PC3 is analogously referred to as resistant *S. aureus.* The bacteria collected through magnetic separation were resuspended in Broth media. AquaSpark Broad Range Phosphatase Substrate (Product Code: A-8197_P00, Biosynth AG, Staad, Switzerland) was in the meanwhile diluted to a concentration of 0.5 mM with Trisma Buffer pH 7.0 containing 1mM $MgCl_2$. 0.196 mL bacterial suspension was subsequently incubated with 4 µL diluted AquaSpark solution for 20min. Luminescence[47] and optical density (OD_{600}) were continuously recorded for 6 hours with a time interval of 0.5 hours using a plate reader (PowerWave HT, BioTek instruments Inc., U.S.A.).

Bacteria-specific capture. The bacterial cultures of *E. coli*, *P. aeruginosa,* susceptible and resistant *S. aureus,* and *S. epidermidis* were diluted with sterile PBS as reported[48-50] to around 10^6 colony forming units $(CFU) \cdot mL^{-1}$. Subsequently, 500 µL bacterial suspension was incubated (for 10 min at 37°C and shaking at 160 rpm) with 50 µL peptide modified PEG@MNCs, 50 µL peptide interacted MNCs, 50 µL PEG@MNCs and 50 µL MNCs, respectively. Then these suspensions were exposed to a magnetic field for 5 min, and the clear supernatant was afterward replaced with fresh 550 µL PBS. This rinsing process was repeated 4 more times. The obtained samples were diluted with fresh PBS, and thereafter 100 µL liquid sample was plated on PC-agar plates with three replicates. The quantification of bacterial colonies on PC-agar plates was performed after incubating the plates at 37°C for 12 hours. This specific capture was analyzed based on different times of the rinsing process: from no rinsing to 5 times rinsing.

Adhesion force analysis between bacteria and nanoclusters.

In order to immobilize MNCs (non-functionalized/functionalized MNCs/PEG@MNCs) on glass-bottom microscopy dishes (GWSB-5040, WillCo-Dish, Amsterdam, Netherlands) for force spectroscopy experiments, 2 mL 9 $g \cdot L^{-1}$ MNCs were precipitated on polydopamine-coated glass. Glass-bottom microscopy dishes were coated with polydopamine as previously reported[28]. Briefly, the bottom glass of the microscopy dishes was cleaned with 2-propanol with sonication and then deionized water. Subsequently, N_2-stream was utilized to dry the cleaned bottom glass of the microscopy dishes before the treatment with air plasma for 2 minutes (Plasma Cleaner PD-32G, Harrick Plasma, USA). 4 mL 4 $g \cdot L^{-1}$ Polydopamine (in 10 mM TRIS HCl, pH 8.5) was added to immerse the cleaned bottom glass for 1 hour before an extensive washing with PBS. The MNCs suspensions were added and interacted with the coated glass surfaces for 60 minutes. Unbounded MNCs were rinsed off with PBS. The attached MNCs were immersed with 4 mL PBS to guarantee a good immersion of the FluidFM setup in the buffer.

The Flex Bio-AFM (Nanosurf, Switzerland) and the digital pressure controller (Cytosurge, Switzerland) were similarly applied as reported[16, 51]. Single-cell force spectroscopy was similarly exerted at room temperature in PBS (pH 7.4) with *E. coli, P. aeruginosa,* susceptible and resistant *S. aureus,* and *S. epidermidis* as reported[51].

Bacterial specific capture rate. The specific capture rate was analyzed similarly to the assay of bacterial specific capture. However, the incubation time of bacterial suspension and each MNC type varied in the range of 5min, 10min, 30min, 60min, 90min, and 120min.

Bacterial specific capture sensitivity. The specific capture sensitivity was analyzed similarly to the assay of bacterial specific capture. However, before incubating each MNCs, the original bacterial suspensions were additionally diluted 10, 100, 1 000, 10 000, 100 000, and 1000 000-fold, respectively.

Bacterial specific capture in human serum. Bacterial specific capture in human serum was similarly performed as in the assay of bacterial specific capture. Bacterial suspension mixtures were prepared as follows with each bacteria of 10^6 CFU·mL^{-1}: susceptible *S. aureus* & *E. coli*, susceptible *S. aureus* & *P. aeruginosa,* susceptible *S. aureus* & *S. epidermidis*, resistant *S. aureus* & *E. coli*, resistant *S. aureus* & *P. aeruginosa,* resistant *S. aureus* & *S. epidermidis,* and susceptible *S. aureus* & resistant *S. aureus*. Moreover, the resistance of the captured bacteria was analyzed, as mentioned above, in the assay of AMR detection.

Polymerase chain reaction (PCR) analysis. Primers (16SSAIII-SA:5'-TATAGATGGATCCGCGCT-3' and 16SSAIV-SA: 5'-GATTAGGTACCGTCAAGAT-3'; forward primer targeting *E. coli*: 5'-CTGCTTCTTTTAAGCAACTGGCGA-3' and reverse primer targeting *E. coli*: 5'-ACCAGACCCAGCACCAGATAAG-3'; FtoxA-PA: 5′-TTCGTCAGGGCGCACGAGAGCA-3′ and RtoxA-PA: 5′-TCTCCAGCGGCAGGTGGCAAG-3′) were applied to amplify the region from the 5' of the upstream to the 3' of the downstream region of 16S rRNA of *S. aureus*. All PCR analyses were exerted using 200 µL captured bacteria as DNA source, 200 µM nucleotides (N0447S, NEB, USA), adequate primers (0.5 µM), 3% DMSO, 1X Buffer Phusion HF, and 1 Unit·mL^{-1} Phusion DNA Polymerase (Phusion High-Fidelity DNA Polymerase, M0530, NEB, USA). Cycling conditions were 98 °C for 360 s, followed by 31 cycles of 98 °C for 10 s, 58 °C for 30 s, and 72°C for 90 s, and a final extension at 72 °C for 300 s. PCR products were separated by electrophoresis at 100 V for 60 minutes in 1% (w/v) agarose gel (V3125, Promega, Spain). The yielded size of every amplicon was aligned to the 1 kb DNA ladder (GeneRuler 1 kb DNA Ladder, SM0333, Thermo Scientific, USA).

ASSOCIATED CONTENT

Supporting Information Available: The following files are available free of charge.

Bacterial capture in PBS without rinsing (Figure S1); Bacterial capture in human serum (Figure S2); Capture specificity to *S. aureus* (Figure S3).

AUTHOR INFORMATION

Corresponding Author

Fei Pan − Laboratory for Biointerfaces, Empa, Swiss Federal Laboratories for Materials Science and Technology, Lerchenfeldstrasse 5, 9014 St. Gallen, Switzerland; orcid.org/0000-0002-9801-5619; Email: Fei.Pan@empa.ch

Qun Ren − Laboratory for Biointerfaces, Empa, Swiss Federal Laboratories for Materials Science and Technology, Lerchenfeldstrasse 5, 9014 St. Gallen, Switzerland; orcid.org/0000-0003-0627-761X; Email: Qun.Ren@empa.ch

Authors

Stefanie Altenried − Laboratory for Biointerfaces, Empa, Swiss Federal Laboratories for Materials Science and Technology, Lerchenfeldstrasse 5, 9014 St. Gallen, Switzerland; orcid.org/0000-0001-7130-8094

Subas Scheibler − Nanoparticle Systems Engineering Laboratory, Institute of Process Engineering, Department of Mechanical and Process Engineering, ETH Zürich, Sonneggstrasse 3, 8092 Zürich, Switzerland; Laboratory for Particles Biology Interactions, Empa, Swiss Federal Laboratories for Materials Science and Technology, Lerchenfeldstrasse 5, 9014 St. Gallen, Switzerland; orcid.org/0000-0003-0425-0026

Irene Rodriguez Fernandez − Laboratory for Biointerfaces, Empa, Swiss Federal Laboratories for Materials Science and Technology, Lerchenfeldstrasse 5, 9014 St. Gallen, Switzerland; orcid.org/0000-0002-8988-4927

Giorgia Giovannini – Laboratory for Biomimetic Membranes and Textiles, Empa Swiss Federal Laboratories for Materials Science and Technology, Lerchenfeldstrasse 5, 9014 St. Gallen, Switzerland; orcid.org/0000-0003-4496-3709

Author contributions

Contribution description

F. Pan and Q. Ren conceptualized, designed, and managed this work. Q. Ren initiated this work and proposed the general idea. F. Pan performed the experiments. This manuscript was prepared by F. Pan, and Q. Ren. S. Altenried contributed her microbiological expertise to the microbiology tests. I. Rodriguez Fernandez contributed to sample preparation and luminescence analysis. S. Scheibler, and G. Giovannini, contributed to the characterization of magnetic nanoclusters.

CRediT author statement

Fei Pan: Conceptualization, Methodology, Software, Validation, Formal analysis, Investigation, Visualization, Supervision, Project administration, Writing - Original Draft, Writing - Review & Editing.

Stefanie Altenried: Methodology, Validation, Investigation.

Subas Scheibler: Methodology, Investigation, Validation.

Irene Rodriguez Fernandez: Methodology, Investigation, Validation.

Giorgia Giovannini: Methodology, Investigation, Validation.

Qun Ren: Conceptualization, Methodology, Validation, Investigation, Supervision, Project administration, Writing - Original Draft, Writing - Review & Editing.

Disclosure Statement and Declaration of Competing Interest

There are no conflicts to declare.

Data availability

The data supporting this study are available from the corresponding authors upon reasonable request.

Acknowledgments

The authors gratefully acknowledge the financial support from Empa for Fei Pan's doctoral research. The authors thank Dr. Mario Hupfeld and Dr. Lukas Tanner from NEMIS Technologies AG (Dübendorf, Switzerland), and Dr. Julian Ihssen from Biosynth AG (Staad, Switzerland) for their kind support and donation of AquaSpark Broad Range Phosphatase Substrate. O. Guillaume-Gentil and Nico Strohmeyer are acknowledged for their kind input concerning FluidFM.

Reference

(1) Kaukonen, K.-M.; Bailey, M.; Pilcher, D.; Cooper, D. J.; Bellomo, R. Systemic inflammatory response syndrome criteria in defining severe sepsis. *New England Journal of Medicine* **2015**, *372* (17), 1629-1638.

(2) Liesenfeld, O.; Lehman, L.; Hunfeld, K.-P.; Kost, G. Molecular diagnosis of sepsis: new aspects and recent developments. *European Journal of Microbiology and Immunology* **2014**, *4* (1), 1-25.

(3) Minasyan, H. Sepsis: mechanisms of bacterial injury to the patient. *Scand J Trauma Resusc Emerg Med* **2019**, *27* (1), 19-19.

(4) Angus, D. C.; Van der Poll, T. Severe sepsis and septic shock. *N Engl J Med* **2013**, *369*, 840-851.

(5) McAdow, M.; Kim, H. K.; DeDent, A. C.; Hendrickx, A. P.; Schneewind, O.; Missiakas, D. M. Preventing Staphylococcus aureus sepsis through the inhibition of its agglutination in blood. *PLoS pathogens* **2011**, *7* (10), e1002307.

(6) Choi, J.; Yoo, J.; Lee, M.; Kim, E.-G.; Lee, J. S.; Lee, S.; Joo, S.; Song, S. H.; Kim, E.-C.; Lee, J. C. A rapid antimicrobial susceptibility test based on single-cell morphological analysis. *Science translational medicine* **2014**, *6* (267), 267ra174.

(7) Nag, P.; Sadani, K.; Mukherji, S.; Mukherji, S. Beta-lactam antibiotics induced bacteriolysis on LSPR sensors for assessment of antimicrobial resistance and quantification of antibiotics. *Sensors and Actuators B: Chemical* **2020**, *311*, 127945.

(8) Loonen, A. J. M.; Bos, M. P.; van Meerbergen, B.; Neerken, S.; Catsburg, A.; Dobbelaer, I.; Penterman, R.; Maertens, G.; van de Wiel, P.; Savelkoul, P.; et al. Comparison of Pathogen DNA Isolation Methods from Large Volumes of Whole Blood to Improve Molecular Diagnosis of Bloodstream Infections. *Plos One* **2013**, *8* (8), e72349.

(9) Boardman, A. K.; Campbell, J.; Wirz, H.; Sharon, A.; Sauer-Budge, A. F. Rapid Microbial Sample Preparation from Blood Using a Novel Concentration Device. *Plos One* **2015**, *10* (2), e0116837.

(10) Bernhardt, M.; Pennell, D. R.; Almer, L. S.; Schell, R. F. Detection of Bacteria in Blood by Centrifugation and Filtration. *J Clin Microbiol* **1991**, *29* (3), 422-425.

(11) Herlich, M. B.; Schell, R. F.; Francisco, M.; Lefrock, J. L. Rapid Detection of Simulated Bacteremia by Centrifugation and Filtration. *J Clin Microbiol* **1982**, *16* (1), 99-102.

(12) Lamberg, R. E.; Schell, R. F.; Lefrock, J. L. Detection and Quantitation of Simulated Anaerobic Bacteremia by Centrifugation and Filtration. *J Clin Microbiol* **1983**, *17* (5), 856-859.

(13) Zelenin, S.; Hansson, J.; Ardabili, S.; Ramachandraiah, H.; Brismar, H.; Russom, A. Microfluidic-based isolation of bacteria from whole blood for sepsis diagnostics. *Biotechnol Lett* **2015**, *37* (4), 825-830.

(14) Raub, C. B.; Lee, C.; Kartalov, E. Sequestration of bacteria from whole blood by optimized microfluidic cross-flow filtration for Rapid Antimicrobial Susceptibility Testing. *Sensor Actuat B-Chem* **2015**, *210*, 120-123.

(15) Boardman, A. K.; Wong, W. S.; Premasiri, W. R.; Ziegler, L. D.; Lee, J. C.; Miljkovic, M.; Klapperich, C. M.; Sharon, A.; Sauer-Budge, A. F. Rapid Detection of Bacteria from Blood with Surface-Enhanced Raman Spectroscopy. *Anal Chem* **2016**, *88* (16), 8026-8035.

(16) Pan, F.; Zhang, S.; Altenried, S.; Zuber, F.; Chen, Q.; Ren, Q. Advanced antifouling and antibacterial hydrogels enabled by the controlled thermo-responses of a biocompatible polymer composite. *Biomaterials Science* **2022**, 10.1039/D2BM01244H.

(17) Guo, F.; Pan, F.; Zhang, W.; Liu, T.; Zuber, F.; Zhang, X.; Yu, Y.; Zhang, R.; Niederberger, M.; Ren, Q. Robust Antibacterial Activity of Xanthan-Gum-Stabilized and Patterned CeO2–x–TiO2 Antifog Films. *ACS Applied Materials & Interfaces* **2022**. DOI: https://doi.org/10.1021/acsami.2c11968

(18) Lesniewski, A.; Los, M.; Jonsson-Niedziolka, M.; Krajewska, A.; Szot, K.; Los, J. M.; Niedziolka-Jonsson, J. Antibody Modified Gold Nanoparticles for Fast and Selective, Colorimetric T7 Bacteriophage Detection. *Bioconjugate Chem* **2014**, *25* (4), 644-648.

(19) Lai, H. Z.; Wang, S. G.; Wu, C. Y.; Chen, Y. C. Detection of Staphylococcus aureus by Functional Gold Nanoparticle-Based Affinity Surface-Assisted Laser Desorption/Ionization Mass Spectrometry. *Anal Chem* **2015**, *87* (4), 2114-2120.

(20) Bohara, R. A.; Pawar, S. H. Innovative Developments in Bacterial Detection with Magnetic Nanoparticles. *Appl Biochem Biotech* **2015**, *176* (4), 1044-1058.

(21) Kang, J. H.; Super, M.; Yung, C. W.; Cooper, R. M.; Domansky, K.; Graveline, A. R.; Mammoto, T.; Berthet, J. B.; Tobin, H.; Cartwright, M. J. An extracorporeal blood-cleansing device for sepsis therapy. *Nature medicine* **2014**, *20* (10), 1211-1216.

(22) Lattuada, M.; Ren, Q.; Zuber, F.; Galli, M.; Bohmer, N.; Matter, M. T.; Wichser, A.; Bertazzo, S.; Pier, G. B.; Herrmann, I. K. Theranostic body fluid cleansing: rationally designed magnetic particles enable capturing and detection of bacterial pathogens. *Journal of Materials Chemistry B* **2016**, *4* (44), 7080-7086.

(23) Bundy, J. L.; Fenselau, C. Lectin and carbohydrate affinity capture surfaces for mass spectrometric analysis of microorganisms. *Analytical Chemistry* **2001**, *73* (4), 751-757.

(24) Adey, N. B.; Mataragnon, A. H.; Rider, J. E.; Carter, J. M.; Kay, B. K. Characterization of phage that bind plastic from phage-displayed random peptide libraries. *Gene* **1995**, *156* (1), 27-31.

(25) Kabir, M. E.; Krishnaswamy, S.; Miyamoto, M.; Furuichi, Y.; Komiyama, T. An improved phage-display panning method to produce an HM-1 killer toxin anti-idiotypic antibody. *BMC biotechnology* **2009**, *9* (1), 1-16.

(26) Yarbrough, D. K.; Hagerman, E.; Eckert, R.; He, J.; Choi, H.; Cao, N.; Le, K.; Hedger, J.; Qi, F.; Anderson, M. Specific binding and mineralization of calcified surfaces by small peptides. *Calcified tissue international* **2010**, *86* (1), 58-66.

(27) Rao, S. S.; Mohan, K. V. K.; Gao, Y.; Atreya, C. D. Identification and evaluation of a novel peptide binding to the cell surface of Staphylococcus aureus. *Microbiological research* **2013**, *168* (2), 106-112.

(28) Mittelviefhaus, M.; Müller, D. B.; Zambelli, T.; Vorholt, J. A. A Modular Atomic Force Microscopy Approach Reveals a Large Range of Hydrophobic Adhesion Forces among Bacterial Members of the Leaf Microbiota. *The ISME journal* **2019**, *13* (7), 1878-1882.

(29) Lowe, S.; O'Brien-Simpson, N. M.; Connal, L. A. Antibiofouling polymer interfaces: poly(ethylene glycol) and other promising candidates. *Polymer Chemistry* **2015**, *6* (2), 198-212.

(30) Zhang, X.; Liu, L.; Liu, R.; Wang, J.; Hu, X.; Yuan, Q.; Guo, J.; Xing, G.; Zhao, Y.; Gao, X. Specific detection and effective inhibition of a single bacterial species in situ using peptide mineralized Au cluster probes. *Science China Chemistry* **2018**, *61* (5), 627-634.

(31) Wei, J.; Wang, R.; Pan, F.; Fu, Z. Polyvinyl Alcohol/Graphene Oxide Conductive Hydrogels via the Synergy of Freezing and Salting Out for Strain Sensors. *Sensors* **2022**, *22* (8), 3015.

(32) Wei, J.; Zhu, C.; Zeng, Z.; Pan, F.; Wan, F.; Lei, L.; Nyström, G.; Fu, Z. Bioinspired cellulose-integrated MXene-based hydrogels for multifunctional sensing and electromagnetic interference shielding. *Interdisciplinary Materials* **2022**, 1-12.

(33) Lai, Y.-S.; Del Rosario, M. A. J. V. G.; Chen, W.-F.; Yen, S.-C.; Pan, F.; Ren, Q.; Su, Y.-H. Energy-Yielding Mini Heat Thermocells with WS2 Water-Splitting Dual System to Recycle Wasted Heat. *ACS Applied Energy Materials* **2019**, *2* (10), 7092-7103.

(34) Anthis, A. H. C.; Matter, M. T.; Keevend, K.; Gerken, L. R. H.; Scheibler, S.; Doswald, S.; Gogos, A.; Herrmann, I. K. Tailoring the Colloidal Stability, Magnetic Separability, and Cytocompatibility of High-Capacity Magnetic Anion Exchangers. *ACS Applied Materials & Interfaces* **2019**, *11* (51), 48341-48351.

(35) Pan, F.; Wu, C.-C.; Chen, Y.-L.; Kung, P.-Y.; Su, Y.-H. Machine learning ensures rapid and precise selection of gold sea-urchin-like nanoparticles for desired light-to-plasmon resonance. *Nanoscale* **2022**, *14*, 13532-13541

(36) Yang, Y.; Wu, N.; Li, B.; Liu, W.; Pan, F.; Zeng, Z.; Liu, J. Biomimetic Porous MXene Sediment-Based Hydrogel for High-Performance and Multifunctional Electromagnetic Interference Shielding. *ACS Nano* **2022**, *16*(9), 15042–15052.

(37) Pan, F.; Chen, H.-L.; Su, Y.-H.; Su, Y.-H.; Hwang, W.-S. Inclusions properties at 1673 K and room temperature with Ce addition in SS400 steel. *Scientific Reports* **2017**, *7*, 2564.

(38) Pan, F.; Su, Y.-H.; Augusto, J.; Hwang, W.-S.; Chen, H.-L. Optical inclusion transformation with different amount of cerium addition during solidification of SS400 steel. *Optical and Quantum Electronics* **2016**, *48* (12), 536.

(39) Kung, P.-Y.; Pan, F.; Su, Y.-H. Spintronic hydrogen evolution induced by surface plasmon of silver nanoparticles loaded on Fe- and Co-doped ZnO nanorods. *Journal of Materials Chemistry A* **2021**, *9* (44), 24863-24873.

(40) Wu, C.-C.; Pan, F.; Su, Y.-H. Surface Plasmon Resonance of Gold Nano-Sea-Urchins Controlled by Machine-Learning-Based Regulation in Seed-Mediated Growth. *Advanced Photonics Research* **2021**, *2* (9), 2100052.

(41) Yu, R.; Pan, F.; Schreine, C.; Wang, X.; Bell, D. M.; Qiu, G.; Wang, J. Quantitative Determination of Airborne Redox-Active Compounds Based on Heating-Induced Reduction of Gold Nanoparticles. *Analytical Chemistry* **2021**, *93* (44), 14859-14868.

(42) Kung, P.-Y.; Pan, F.; Su, Y.-H. Gold Nanoparticles on TM:ZnO (TM: Fe, Co) as Spinplasmon-Assisted Electro-Optic Reaction Modulator in Solar-to-Hydrogen Water Splitting Cell. *ACS Sustainable Chemistry & Engineering* **2020**, *8* (39), 14743-14751.

(43) Tseng, M.-Y.; Su, Y.-H.; Lai, Y.-S.; Pan, F.; Kung, P.-Y. Cobalt−Citrate Metal−Organic-Framework UTSA-16 on TiO2 Nanoparticles. *IOP Conference Series: Materials Science and Engineering* **2020**, *720*, 012008.

(44) Jin, G.; Prabhakaran, M. P.; Kai, D.; Annamalai, S. K.; Arunachalam, K. D.; Ramakrishna, S. Tissue engineered plant extracts as nanofibrous wound dressing. *Biomaterials* **2013**, *34* (3), 724-734.

(45) Solar, P.; González, G.; Vilos, C.; Herrera, N.; Juica, N.; Moreno, M.; Simon, F.; Velásquez, L. Multifunctional polymeric nanoparticles doubly loaded with SPION and ceftiofur retain their physical and biological properties. *Journal of Nanobiotechnology* **2015**, *13* (1), 14.

(46) Pan, F.; Giovannini, G.; Zhang, S.; Altenried, S.; Zuber, F.; Chen, Q.; Boesel, L. F.; Ren, Q. pH-responsive silica nanoparticles for triggered treatment of skin wound infections. *Acta Biomaterialia* **2022**, *145*, 172-184.

(47) Lai, Y.-S.; Pan, F.; Su, Y.-H. Firefly-like Water Splitting Cells Based on FRET Phenomena with Ultrahigh Performance over 12%. *ACS Applied Materials & Interfaces* **2018**, *10* (5), 5007-5013.

(48) Pan, F.; Altenried, S.; Zuber, F.; Wagner, R. S.; Su, Y.-H.; Rottmar, M.; Maniura-Weber, K.; Ren, Q. Photo-activated Titanium Surface Confers Time Dependent Bactericidal Activity towards Gram Positive and Negative Bacteria. *Colloids and Surfaces B: Biointerfaces* **2021**, *206*, 111940.

(49) Pan, F.; Amarjargal, A.; Altenried, S.; Liu, M.; Zuber, F.; Zeng, Z.; Rossi, R. M.; Maniura-Weber, K.; Ren, Q. Bioresponsive Hybrid Nanofibers Enable Controlled Drug Delivery through Glass Transition Switching at Physiological Temperature. *ACS Applied Bio Materials* **2021**, *4* (5), 4271-4279.

(50) Pan, F.; Altenried, S.; Liu, M.; Hegemann, D.; Bülbül, E.; Moeller, J.; Schmahl, W. W.; Maniura-Weber, K.; Ren, Q. A Nanolayer Coating on Polydimethylsiloxane Surfaces Enables a Mechanistic Study of Bacterial Adhesion Influenced by Material Surface Physicochemistry. *Materials Horizons* **2020**, *7* (1), 93-103.

(51) Pan, F.; Liu, M.; Altenried, S.; Lei, M.; Yang, J.; Straub, H.; Schmahl, W. W.; Maniura-Weber, K.; Guillaume-Gentil, O.; Ren, Q. Uncoupling Bacterial Attachment on and Detachment from Polydimethylsiloxane Surfaces through Empirical and Simulation Studies. *Journal of Colloid and Interface Science* **2022**, *622*, 419-430.

Figures

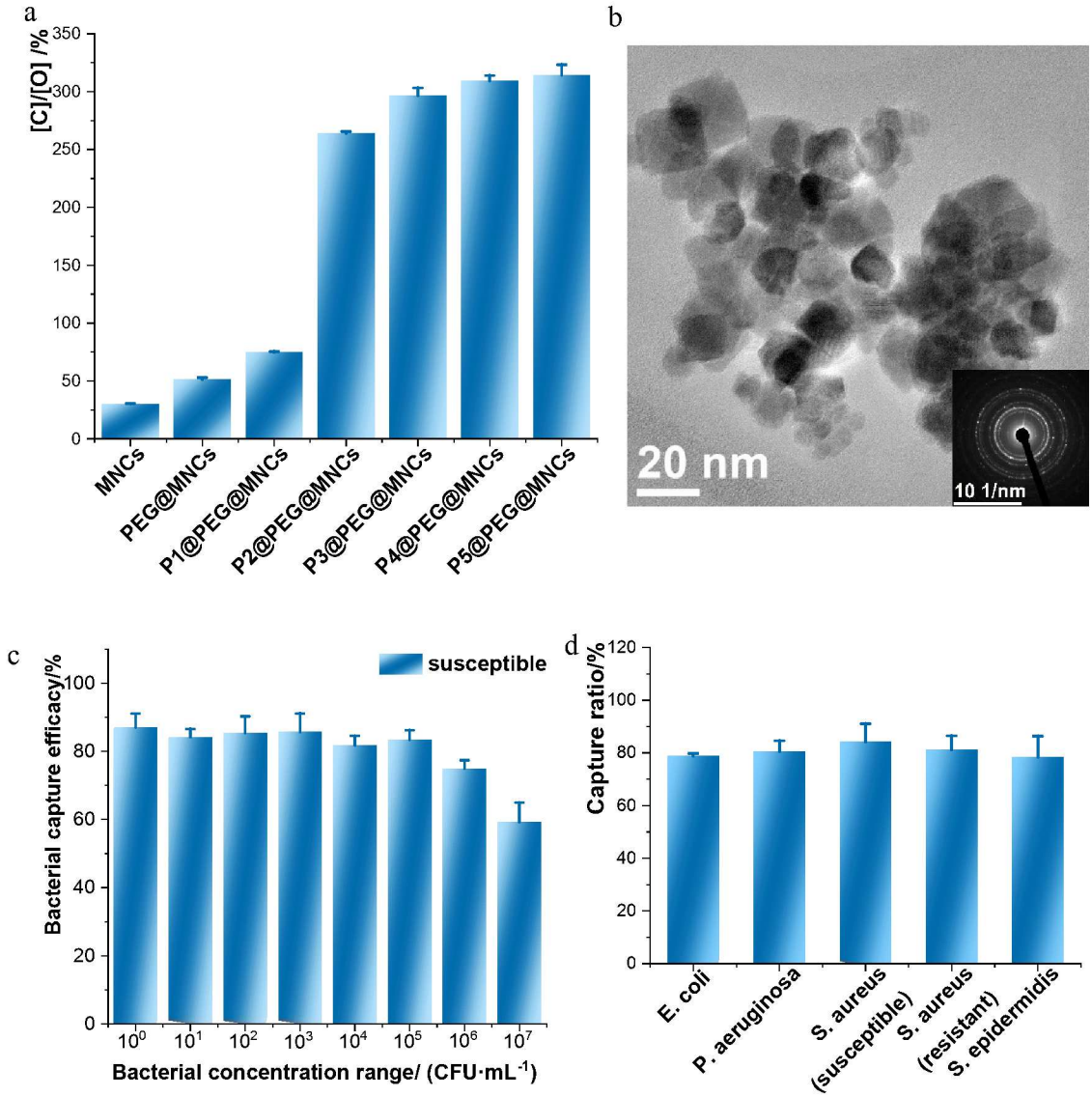

Figure 1. Characterization of the functionalized MNCs and their capture capability towards bacteria without the rinsing process. (a) The elemental ratio [C]/[O] was analyzed through XPS to understand the modification efficiency of PEGylated MNCs by the peptide solutions of different concentrations. P1-P5 represented respectively peptide solutions of 0.02, 0.2, 1, 2 and 20 mM. (b) PEGylated MNCs functionalized by peptide solution of 2 mM (peptide@PEG@MNCs) were imaged using a scanning transmission electron microscope (STEM) which shows a cluster structure of the particles composing the MNCs confirmed by the respective electron diffraction pattern in the inset. (c) Capture capability analysis of the functionalized MNCs was performed towards susceptible *S. aureus* of different orders of magnitude of concentrations and normalized to the bacterial concentration of the initial bacterial suspension at every order of magnitude (an initial bacterial suspension of 71900000 ± 800000 CFU·mL^{-1} was considered as the magnitude of 10^7 CFU·mL^{-1}, and the rest from 10^6-10^0 CFU·mL^{-1} was stepwise one magnitude lower than the bacterial suspension of 10^7 CFU·mL^{-1}). (d) Capture efficiencies of peptide@PEG@MNCs without rinsing process towards *E. coli*, *P.*

aeruginosa, susceptible and resistant *S. aureus,* and *S. epidermidis* were respectively normalized to the initial suspension of 398000 ± 10000, 580000 ± 30000, 890000 ± 20000, 159000 ± 9000, and 569000 ± 23000 CFU·mL^{-1}. N = 3 (biological repeats), mean ± SD shown; at least two sets of independent experiments were performed, and one set of data is displayed here.

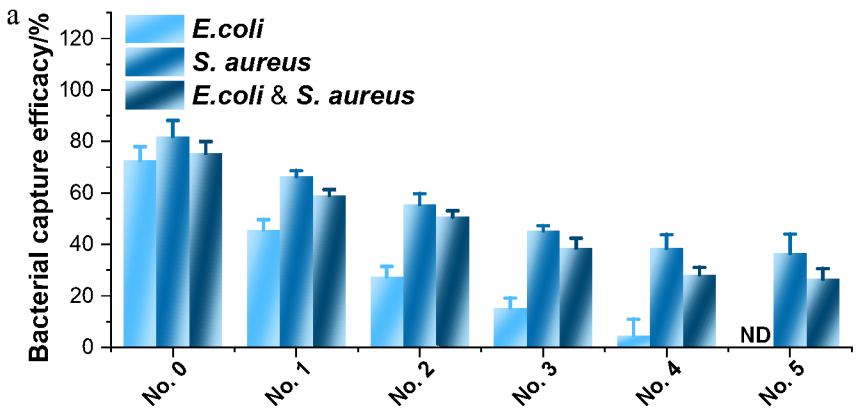

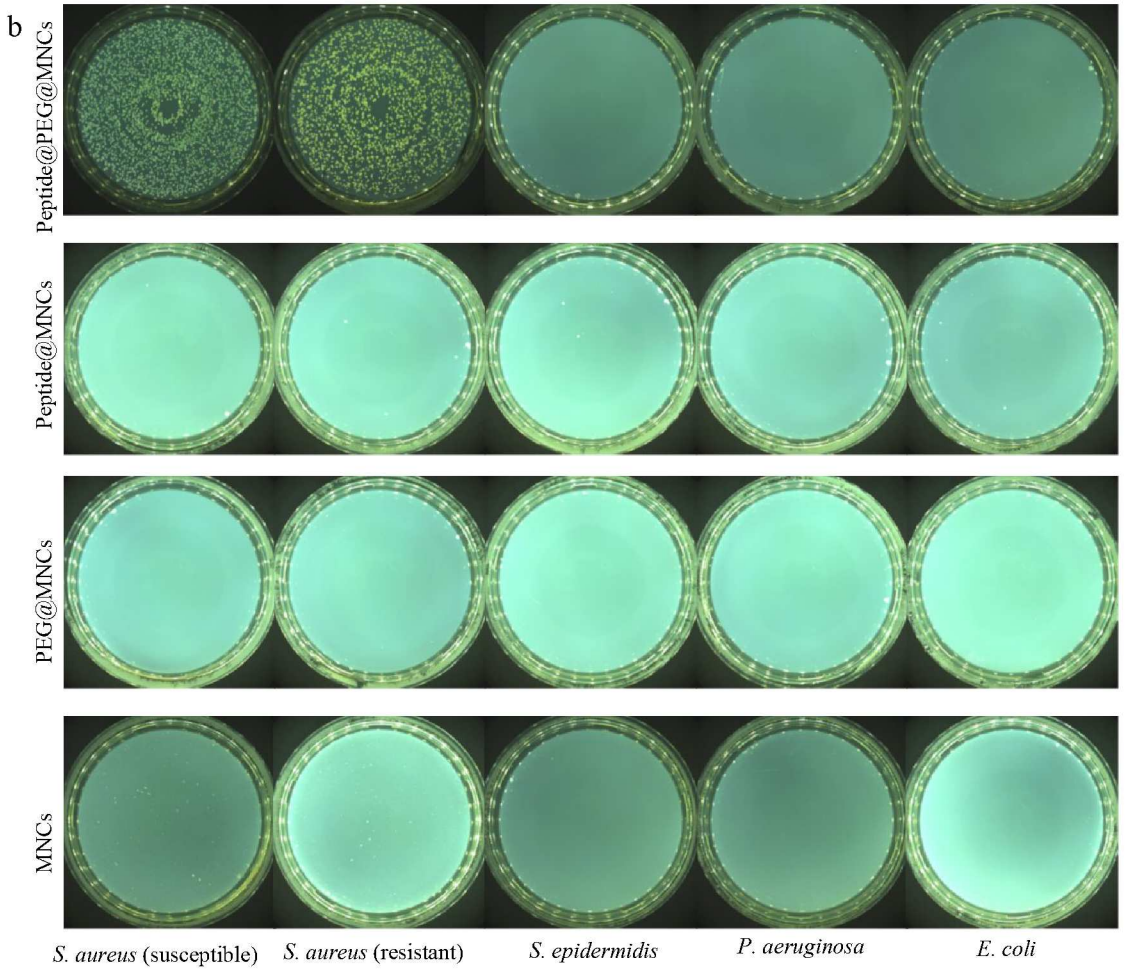
b
Peptide@PEG@MNCs
Peptide@MNCs
PEG@MNCs
MNCs
S. aureus (susceptible)
S. aureus (resistant)
S. epidermidis
P. aeruginosa
E. coli

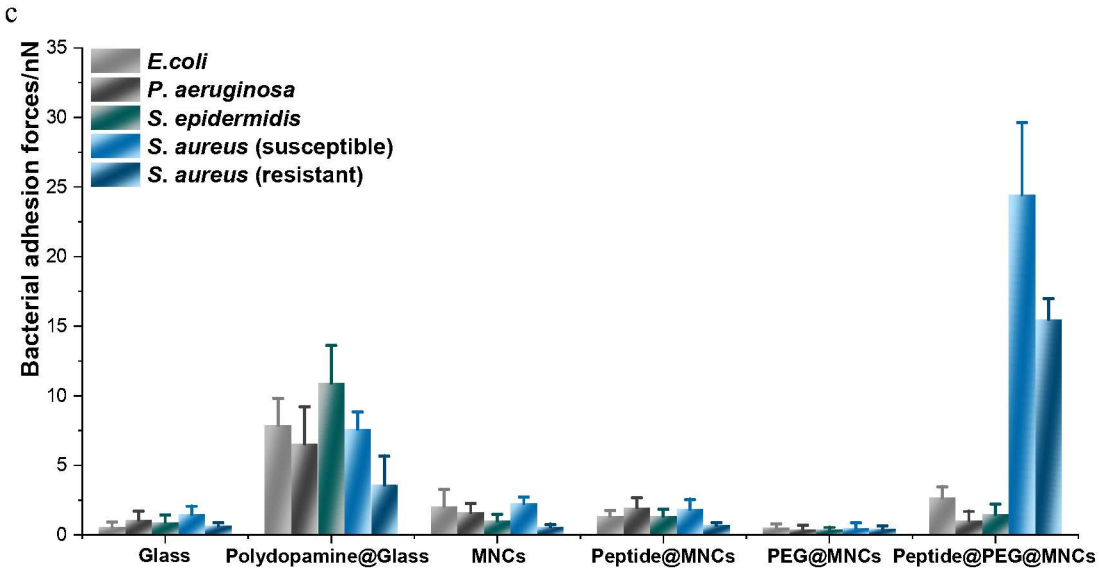
c
Bacterial adhesion forces/nN
E.coli
P. aeruginosa
S. epidermidis
S. aureus (susceptible)
S. aureus (resistant)
0
5
10
15
20
25
30
35
Glass
Polydopamine@Glass
MNCs
Peptide@MNCs
PEG@MNCs
Peptide@PEG@MNCs

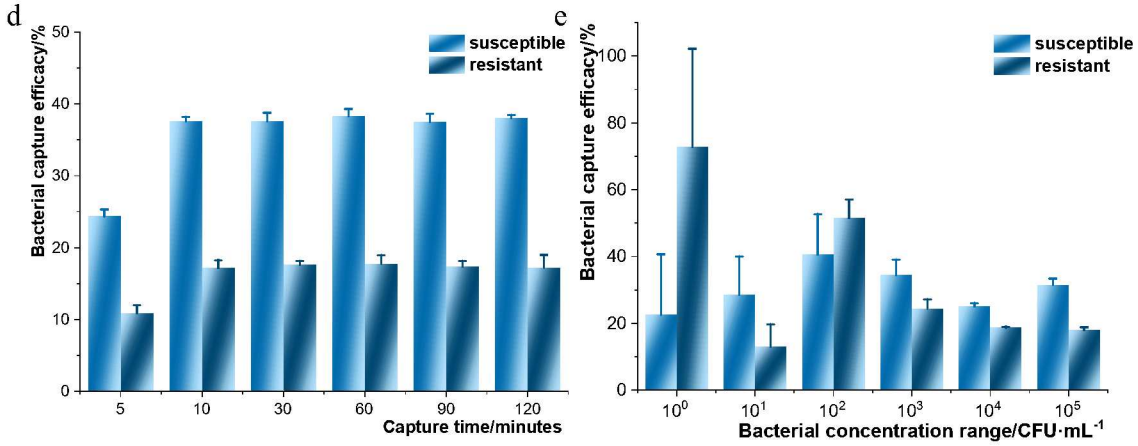

Figure 2. Specific bacterial capture in PBS with a rinsing process. (a) Captured bacteria through functionalized MNCs were sequentially rinsed up to 5 times to yield a specific capture of *S. aureus*. No was termed as no rinsing, and No. 1 - No. 5 were termed as the rinsing times. The capture efficacy from the mixed bacterial strains was aligned with the sum of initial *E. coli* and susceptible *S. aureus*. Initial concentrations of *E. coli* and *S. aureus* were 228000 ± 25000 and 590000 ± 20000 CFU·mL^{-1}, respectively. (b) Specific bacterial capture through the MNCs, PEG@MNCs, peptide@MNCs, and peptide@PEG@MNCs towards susceptible and resistant *S. aureus*, *S. epidermidis*, *P. aeruginosa,* and *E. coli*. (c) Affinity evaluation between bacteria and functionalized/non-functionalized MNCs through single bacterial force spectroscopy. Functionalized/non-functionalized MNCs were deposited on glass petri dishes coated with polydopamine according to published methods[28]. (d) Assessment of bacterial capture rate through the functionalized PEG@MNCs was performed to interact 5, 10, 30, 60, 90, and 120 min towards susceptible and resistant *S. aureus*. The bacterial concentrations of initial bacterial suspension are respectively 433000 ± 152000 and 480000 ± 10000 CFU·mL^{-1} for susceptible and resistant *S. aureus*. (e) Evaluation of bacterial capture sensitivity by the functionalized PEG@MNCs towards suspension of susceptible and resistant bacteria at concentrations of various concentration ranges: 10^5-10^0 CFU·mL^{-1}, which were stepwise diluted by 10 fold till reaching a concentration range of 10^0 CFU·mL^{-1} from the bacterial suspension in a concentration range of 10^5 CFU·mL^{-1}. The bacterial concentrations of initial bacterial suspension are 443000 ± 5000 and 485000 ± 13000 CFU·mL^{-1} for susceptible and resistant *S. aureus*, respectively. n = 3 (biological repeats), mean ± SD shown, for (a), and (d)&(e).

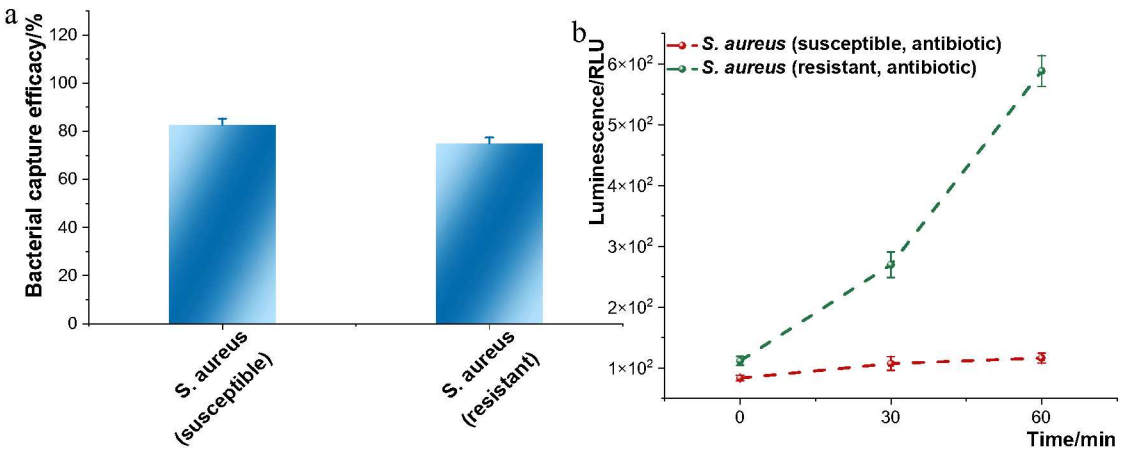

c

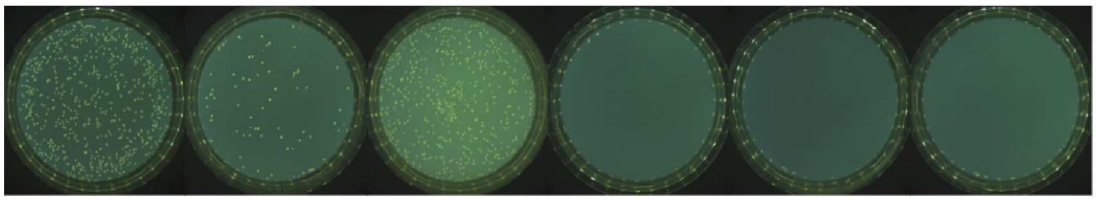

S. aureus (susceptible) | *S. aureus* (resistant) | *S. aureus* (susceptible & resistant) | *S. epidermidis* | *P. aeruginosa* | *E. coli*

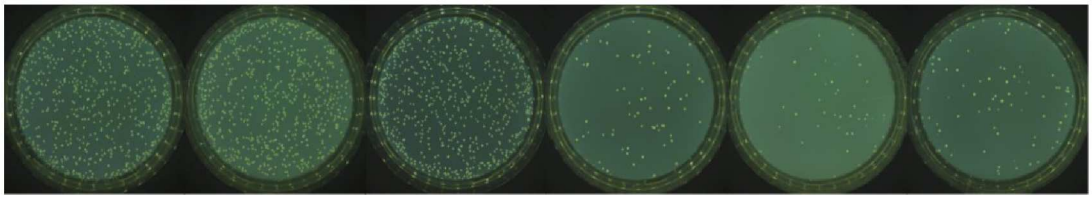

S. epidermidis & *S. aureus* (susceptible) | *P. aeruginosa* & *S. aureus* (susceptible) | *E. coli* & *S. aureus* (susceptible) | *S. epidermidis* & *S. aureus* (resistant) | *P. aeruginosa* & *S. aureus* (resistant) | *E. coli* & *S. aureus* (resistant)

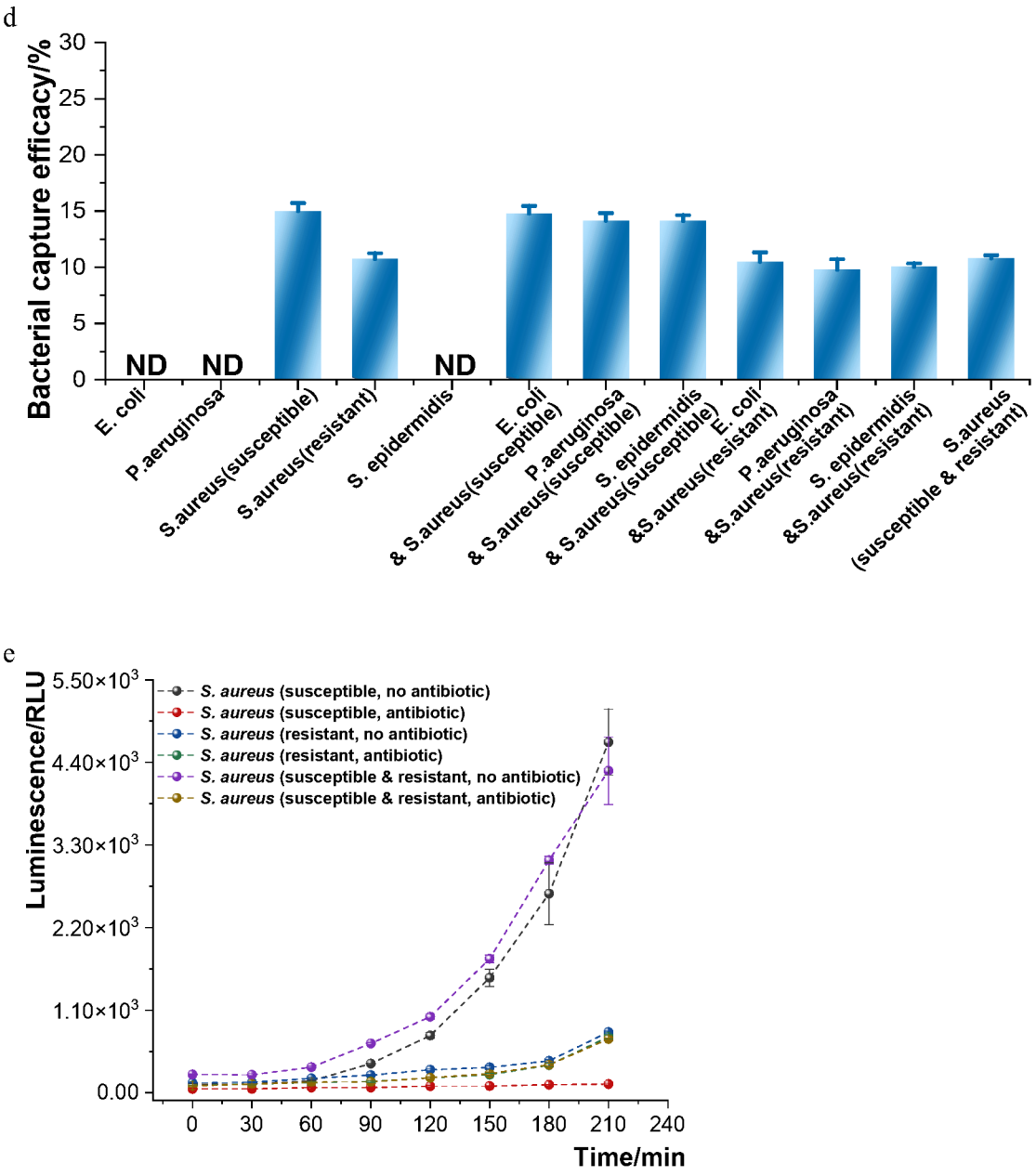

Figure 3. Bacterial capture in human serum. (a) Capture efficiencies of the peptide@PEG@MNCs without rinsing process towards susceptible and resistant *S. aureus* normalized to the respective initial suspension of 939000 ± 14000 and 445000 ± 26000CFU·mL^{-1}. (b) Bacterial growth of the captured susceptible and resistant *S. aureus* was analyzed with and without the presence of 5 μg·mL^{-1} vancomycin through AquaSpark Broad Range Phosphatase Substrate. (c) Specific bacterial capture through the peptide@PEG@MNCs towards susceptible and resistant *S. aureus*, *S. epidermidis*, *P. aeruginosa,* and *E. coli*, and susceptible and resistant *S. aureus,* mixed with *S. epidermidis*, *P. aeruginosa,* and *E. coli,* respectively. (d) Specific bacterial capture efficiencies through the peptide@PEG@MNCs towards susceptible and resistant *S. aureus*, *S. epidermidis*, *P. aeruginosa,* and *E. coli*, and susceptible and resistant *S. aureus,* mixed with *S. epidermidis*, *P. aeruginosa,* and *E. coli*, respectively. Capture towards single bacterial strains was normalized to its initial bacterial

concentration (susceptible *S. aureus*: 437000 ± 20000 CFU·mL^{-1}, resistant *S. aureus:* 169000 ± 24000 CFU·mL^{-1}, *S. epidermidis*: 1600000 ± 278000 CFU·mL^{-1}, *P. aeruginosa*: 500000 ± 87000 CFU·mL^{-1} and *E. coli*: 366000 ± 6000 CFU·mL^{-1}). Capture towards bacterial mixtures was respectively aligned to susceptible *S. aureus* once in the presence of susceptible *S. aureus* and resistant *S. aureus* once in the presence of resistant *S. aureus* except for the mixture of susceptible and resistant *S. aureus*, which was aligned to the sum of the initial bacterial concentrations of susceptible and resistant *S. aureus*. (e) Bacterial growth of the specifically captured bacteria was analyzed with and without the presence of 5 μg·mL^{-1} vancomycin through AquaSpark Broad Range Phosphatase Substrate. n = 3 (biological repeats), mean ± SD shown.

Table

Table 1. Affinity evaluation between bacteria and functionalized/non-functionalized MNCs through single bacterial force spectroscopy. Functionalized/non-functionalized MNCs were deposited on glass petri dishes coated with polydopamine according to published methods[28]

Single bacterial adhesion force between different bacterial pathogens and various surfaces/nN					
	E. coli	*P. aeruginosa*	*S. epidermidis*	Susceptible *S. aureus*	Resistant S. *aureus*
Glass	0.58 ± 0.33	1.08 ± 0.62	0.93 ± 0.49	1.48 ± 0.57	0.66 ± 0.22
polydopamine@Glass	7.88 ± 1.93	6.56 ± 2.64	10.92 ± 2.69	7.61 ± 1.21	3.60 ± 2.07
MNCs	2.06 ± 1.21	1.61 ± 0.64	1.03 ± 0.43	2.28 ± 0.44	0.59 ± 0.16
Peptide@MNCs	1.36 ± 0.40	1.97 ± 0.70	1.37 ± 0.48	1.86 ± 0.69	0.70 ± 0.17
PEG@MNCs	0.54 ± 0.24	0.42 ± 0.27	0.41 ± 0.12	0.47 ± 0.40	0.44 ± 0.21
Peptide@PEG@MNCs	2.69 ± 0.78	1.04 ± 0.65	1.49 ± 0.71	24.46 ± 5.18	15.50 ± 1.47

For Table of Contents Only